Analysis of recent η photoproduction data

A. Sibirtsev[1,2,3,4], J. Haidenbauer[3,5], S. Krewald[3,5] and U.-G. Meißner[1,3,5]

[1] Helmholtz-Institut für Strahlen- und Kernphysik (Theorie) und Bethe Center for Theoretical Physics, Universität Bonn,
D-53115 Bonn, Germany
[2] Excited Baryon Analysis Center (EBAC), Thomas Jefferson National Accelerator Facility, Newport News, Virginia 23606,
USA
[3] Institut für Kernphysik and Jülich Center for Hadron Physics, Forschungszentrum Jülich, D-52425 Jülich, Germany
[4] Institute of High Energy Physics and Center for Theoretical Studies, Chinese Academy of Sciences, Beijing 100049, China
[5] Institute for Advanced Simulation, Forschungszentrum Jülich, D-52425 Jülich, Germany

Abstract. Recent data on η-meson photoproduction off a proton target in the energy range $2 \leq \sqrt{s} \leq 3$ GeV
are analyzed with regard to their overall consistency. Results from the ELSA and CLAS measurements are
compared with predictions of a Regge model whose reaction amplitude was fixed via a global fit to pre-2000
measurements of differential cross sections and polarization observables for $\gamma p \to \eta p$ at higher energies. We
find that all recent experimental results on differential cross sections for η-meson photoproduction are in
good agreement with each other, except for the CLAS data from 2009. However, the latter can be made
consistent with the other data at the expense of introducing an energy-dependent renormalization factor.
We point out that there indications in the data for a possible excitation of baryon resonances with masses
around 2.1 and 2.4 GeV.

PACS. 11.55.Jy Regge formalism – 13.60.Le Meson production – 13.60.-r Photon and charged-lepton
interactions with hadrons – 25.20.Lj Photoproduction reactions

1 Introduction

Recently data on $\gamma p \to \eta p$ differential cross sections were
published by the ELSA [1] and CLAS Collaborations [2].
It turned out that there is a substantial disagreement
between the two measurements. In fact, as indicated in
Refs. [1,2], the experimental results were cross checked ap-
plying various methods but no plausible reason was found
for the discrepancy. The status of the data remains the
same - they are inconsistent.

This situation is rather unsatisfactory. The data from
both measurements are given with high statistical and sys-
tematic accuracy and with small increments in energy and
angle. The ELSA measurement covers invariant collision
energies up to $\sqrt{s} \simeq 2.37$ GeV, while the highest energy
considered in the CLAS experiment is $\sqrt{s} = 2.795$ GeV.
Therefore, these new data would allow to study possible
excitation of high-mass baryons. The ηN state couples
to baryons with isospin 1/2 and it might be that η-meson
photoproduction is more selective to resonance excitations
than pion photoproduction or πN scattering. A typical
example is the $P_{11}(1710)$ resonance that was not seen in
many analyses of elastic πN scattering but appears to be-
come very important once one includes the $\pi N \to \eta N$
channel [3] and works in a coupled-channel formalism, see
also the combined analysis of πN scattering and photo-
production data in [4].

For reactions where a large data base exists one can
formulate rejection criteria for inconsistent data sets solely
based on statistical arguments. This was done, for exam-
ple, in partial wave analyses of the NN [5] and $\bar{N}N$ sys-
tems [6]. Unfortunately, for the reaction $\gamma p \to \eta p$ one is far
away from such a situation. Here, one simply would have
to exclude one or the other measurement from the global
data analysis without clear criterion. Apparently, such a
procedure is not very appealing and, moreover, disregards
the experimental progress in studying the spectrum of ex-
cited baryons. In any case, as an alternative, one should
examine whether floating the normalization of some exper-
imental results is a possible way to resolve inconsistencies
between the data. Even in the analysis of reactions with a
large data base, like NN or πN, it is standard practice to
allow for some variation in the normalization of data sets
[5,7,8].

A direct comparison of the different $\gamma p \to \eta p$ measure-
ments is complicated because, in general, data were taken
at different energies and different angles in the ELSA and
CLAS experiments. One possibility is to compare the ob-
served differential cross sections with model predictions.
Phenomenological analyses along this line were presented
in Refs. [9,10] in an attempt to examine the consistency
of $K\Lambda$ photoproduction data. It is clear that any cho-
sen specific model might not be able to describe the data

fully satisfactorily and, thus, will deviate necessarily from the data to some extent. However, one expects that any such deviation between the model calculation and different measurements would occur systematically and on a similar quantitative level if the experimental results are mutually consistent. In the present paper we adopt this idea [9, 10] and perform an analysis of the reaction $\gamma p {\rightarrow} \eta p$ in the same spirit. Specifically, we compare the results from the ELSA and CLAS measurements with predictions of a Regge model [11] whose reaction amplitude was fixed via a global fit to pre-2000 measurements of differential cross sections and polarizations for $\gamma p {\rightarrow} \eta p$ at higher energies, i.e. at photon energies above 3 GeV ($\sqrt{s} >$2.55 GeV).

Apart from analyzing the consistency of the data from different measurements we are also interested in the search for excited baryons with masses above 1.9 GeV. Indeed, possible signals for the excitation of baryon resonances at $\sqrt{s} \geq$1.9 GeV were discussed in the first CLAS publication [12] on η-meson photoproduction. Furthermore, the systematic study of single-pion photoproduction presented in [13,14] indicates also possible signals for resonances at invariant energies around 2 GeV.

There are few excited baryons with a mass above 1.9 GeV listed by the Particle Data Group (PDG) [15] that possibly couple to the ηN channel. These resonances are the $S_{11}(2090)$, the $P_{11}(2110)$ and the $G_{17}(2190)$. They were found in multichannel analyses [16,17]. It is important to note that in Ref. [16] the objective was to evaluate the resonance parameters from available pion-nucleon partial wave analyses (PWA). The issue of extracting such partial wave amplitudes from the observables was not considered in this paper. The evaluation procedure adopted in Ref. [17] is based on a multi-resonance model fitted to available partial waves obtained from πN scattering data. Therefore, the presently available PDG information [15] concerning excited high-mass baryons coupled to the ηN-channel is essentially based on PWA's of pion-nucleon scattering data [18,19,20].

The paper is organized as follows. In Sect. 2 we describe in detail the reaction amplitudes employed in the present investigation. An analysis of the experimental results from ELSA and CLAS is provided in Sects. 3 and 4, respectively. In Sect. 5 we review the current status of the data available for the $\gamma p {\rightarrow} \eta p$ differential cross section and we investigate the consistency of those data in detail. The paper ends with a short summary. Quantitative results of the comparision of the different measurements with the predictions of our Regge model are summarized in an Appendix.

2 The reaction amplitude

Similar to our previous analyses of charged and neutral pion photoproduction [13,21] we use a gauge invariant Regge model, which combines the Regge pole and cut amplitudes for ρ, ω and b_1 exchanges. At high energies the interactions before and after the basic Regge pole exchange mechanisms are essentially elastic or diffractive scattering described by Pomeron exchange. Such a scenario can be

Table 1. Correspondence between t-channel pole exchanges and the helicity amplitudes F_i (i=1,...,3). Here P is the parity, J the spin, I the isospin, G the G-parity, $\mathcal{N}$ the naturalness, and $\mathcal{S}$ the signature factor.

F_i	P	J	I	G	$\mathcal{N}$	$\mathcal{S}$	Exchange
F_1	-1	1	1	+1	+1	-1	ρ
F_1	-1	1	0	-1	+1	-1	ω
F_2	+1	1	1	+1	-1	-1	b_1
F_3	-1	1	1	+1	+1	-1	ρ
F_3	-1	1	0	-1	+1	-1	ω

related to the distorted wave approximation and provides a well defined formulation for constructing Regge cut amplitudes.

We use the t-channel parity conserving helicity amplitudes F_i (i=1,...,4). Here F_1 and F_2 are the natural and unnatural spin-parity t-channel amplitudes to all orders in s, respectively. F_3 and F_4 are the natural and unnatural t-channel amplitudes to leading order in s.

Each Regge pole helicity amplitude is parameterized by

$$F(s,t) = \pi\beta(t)\frac{1+\mathcal{S}\exp[-i\pi\alpha(t)]}{\sin[\pi\alpha(t)]\ \Gamma[\alpha(t)]}\left[\frac{s}{s_0}\right]^{\alpha(t)-1}, \quad (1)$$

where s is the invariant collision energy squared, t is the four-momentum transfer squared and s_0=1 GeV^2 is a scaling parameter. Furthermore, $\beta(t)$ is a residue function, $\mathcal{S}$ is the signature factor and $\alpha(t)$ is the Regge trajectory.

The structure of the vertex function $\beta(t)$ of Eq. (1) is defined by the quantum numbers of the particles at the interaction vertex, similar to the usual particle-exchange Feynman diagrams.

Both natural and unnatural parity particles can be exchanged in the t-channel. The naturalness $\mathcal{N}$ for natural ($\mathcal{N}$=+1) and unnatural ($\mathcal{N}$=−1) parity exchanges is defined as

$$\mathcal{N} = +1 \ \text{if} \ P = (-1)^J,$$
$$\mathcal{N} = -1 \ \text{if} \ P = (-1)^{J+1}, \quad (2)$$

where P and J are the parity and spin of the exchanged particle, respectively. Furthermore, in Regge theory each exchange is denoted by a signature factor $\mathcal{S}$=±1 defined as [22,23]

$$\mathcal{S} = P \times \mathcal{N} = (-1)^J, \quad (3)$$

which enters in Eq. (1).

In the $\gamma p {\rightarrow} \eta p$ reaction there is no difference between the ρ and ω-exchanges if their trajectories are the same. Thus, in some previous studies both contributions were subsummed into a single amplitude. However, in our study we treat ρ and ω exchanges separately, because differences in the two amplitudes might play role in describing observables [24,25,26]. Specifically, this allows us to account for the difference between $\gamma n {\rightarrow} \eta n$ and $\gamma p {\rightarrow} \eta p$ observables because for these reactions the contributions from isoscalar

and isovector exchanges enter with different sign. The contribution of the ρ and ω-exchanges to the reaction amplitudes F_i are given in Table 1, together with the relevant quantum numbers. Both ρ and ω have natural parity and contribute to F_1 and F_3.

It was argued [25] that the photon beam asymmetry would be predominantly $\Sigma=+1$, if there are no other contributions besides ρ/ω exchange. Note, however, that Σ vanishes at forward and backward directions. This can be easily understood while considering the relations between the observables and the t-channel parity conserving helicity amplitudes given in Refs. [21,13]. Experimental data [27,28] available at photon energies of 2.5 and 4 GeV show that the beam asymmetry depends on t. Therefore, one needs additional ingredients that contribute to the unnatural-parity amplitudes F_2 or F_4.

The contribution to F_2 is given by the leading b_1 trajectory, which we also used in the analysis of neutral and charged pion photoproduction. Table 1 shows the contribution of the b_1-exchange. As we discussed in Ref. [21], the information about trajectories that might contribute to the F_4 amplitude is very poor. Thus, in the analyses of the neutral and charged pion photoproduction we neglected this amplitude. For the same reason we decided to neglect F_4 also in the present study.

The trajectories are assumed to be of linear form

$$\alpha(t) = \alpha_0 + \alpha' t , \qquad (4)$$

where the intercept α_0 and the slope α' for the ρ, ω and b_1 trajectories are taken over from analyses of other reactions [21,22,29,30,31]. In particular, for all three trajectories we adopt the slope $\alpha'=0.8$ GeV^{-2}. The values utilized for the intercepts are $\alpha_0=0.53$ for ρ, 0.46 for ω, and 0.51 for the b_1 trajectory.

The residue functions $\beta(t)$ used in our analysis are compiled in Table 2. They are similar to the ones used in some of the previous analyses [24,32,13].

In defining the Regge cut amplitudes we use the following parameterization based on the absorption model [23, 24,33,34,35]

$$F(s,t) = \frac{\pi \beta(t)}{\log(s/s_0)} \frac{1+\mathcal{S}\exp[-i\pi\alpha_c(t)]}{\sin[\pi\alpha_c(t)]\,\Gamma[\alpha_c(t)]} \left[\frac{s}{s_0}\right]^{\alpha_c(t)-1}, \quad (5)$$

with the trajectories defined by

$$\alpha_c = \alpha_0 + \frac{\alpha'\alpha'_P t}{\alpha' + \alpha'_P} , \qquad (6)$$

where α_0 and α' are taken from the pole trajectory given by Eq. (4), and $\alpha'_P=0.2$ GeV^{-2} is the slope of the pomeron trajectory. The specific form of the residue functions $\beta(t)$ to be used in Eq. (5) is given in Table 2.

The relation between the differential cross section analyzed in our study and the t-channel helicity amplitudes is given by

$$\frac{d\sigma}{dt} = \frac{1}{32\pi} \left[\frac{t|F_1|^2 - |F_3|^2}{(t-4m^2)} + |F_2|^2 - t|F_4|^2 \right]. \qquad (7)$$

Table 2. Parameterization of the residue functions $\beta(t)$ for the amplitudes F_i, ($i=1,...,3$). Here c_{ij} is the coupling constant, where the double index refers to the amplitude i and the type of exchange j, as specified in the Table.

	$\beta(t)$	Exchange	j
		Pole amplitudes	
F_1	c_{11}	ρ	1
F_1	c_{12}	ω	2
F_2	$c_{23}\,t$	b_1	3
F_3	$c_{31}\,t$	ρ	1
F_3	$c_{32}\,t$	ω	2
		Cut amplitudes	
F_1	$c_{14}\exp[d_4 t]$	ρ	4
F_1	$c_{15}\exp[d_5 t]$	ω	5
F_1	$c_{16}\exp[d_6 t]$	b_1	6
F_2	$c_{24}\,t\exp[d_4 t]$	ρ	4
F_2	$c_{25}\,t\exp[d_5 t]$	ω	5
F_2	$c_{26}\,t\exp[d_6 t]$	b_1	6
F_3	$c_{34}\,t\exp[d_4 t]$	ρ	4
F_3	$c_{35}\,t\exp[d_5 t]$	ω	5
F_3	$c_{36}\,t\exp[d_6 t]$	b_1	6

Table 3. Parameters of the model. The c_{ij}'s are the coupling constants for the i-th amplitude and the exchange of particle j while the d_j's are exponents appearing in the Regge cut amplitude, cf. Table 2.

j	c_{1j} [$\sqrt{\mu\text{b}}$/GeV]	c_{2j} [$\sqrt{\mu\text{b}}$/GeV^3]	c_{3j} [$\sqrt{\mu\text{b}}$/GeV^2]	d_j [GeV^{-2}]
1	-10.71	–	-1.55	–
2	-5.59	-	-18.05	-
3	-	11.80	–	–
4	275.47	30.57	-31807	0.16
5	-94.71	-35.97	129.14	1.53
6	-306.89	-32.46	331.94	0.12

The invariant collision energy squared, s, and the photon energy E_γ are related by

$$s = m_N^2 + 2m_N E_\gamma, \qquad (8)$$

where m_N is the nucleon mass.

The parameters of our Regge model were fixed by a fit to data on η-meson photoproduction data published before 1982 [11]. Specifically, this concerns the differential cross sections collected at SLAC [36], DESY [37], Cornell [38] and at the Daresbury laboratory [27]. All these measurements were done at and above photon energies of $E_\gamma=2.5$ GeV, which corresponds to an invariant collision energies larger than $\sqrt{s}\simeq2.36$ GeV. In the actual fit only data taken at $E_\gamma\geq3$ GeV were used. In addition we include into the fit procedure the experimental results [27,28] for beam and target asymmetries available at $E_\gamma=3$ GeV and 4 GeV. These polarization data were collected at the Daresbury Laboratory. The values of the model parameters are summarized in Table. 3.

A comparison between those experimental results [36, 37, 38, 27, 28] and our calculation was presented in Ref. [11]. We limited our analysis to the range $|t| \leq 2$ GeV^2. Based on our experience in applying Regge phenomenology to the analysis of different reactions in the past, we expect that Regge works rather well in this t region. Furthermore, most of the data available are within this range.

In the near-forward direction of the $\gamma p \to \eta^0 p$ reaction there is an interference of the F_1 amplitude with the one-photon exchange amplitude, known as Primakoff effect [39], which allows one to determine the $\eta \to \gamma\gamma$ decay width. The Regge model described here has been used by us in Ref. [11] for a study on the Primakoff effect in η-meson photoproduction.

3 ELSA measurements

The $\gamma p \to \eta p$ differential cross section obtained at ELSA in three different experiments [1, 40, 41] are shown in Figs. 1-4 as a function of the four-momentum transfer squared. It can be seen that there is excellent consistency between the three measurements. Note that the 2005 and 2009 measurements [1, 40] were done on a proton target, while the data from 2008 [41] were obtained from quasi-free photoproduction of η-mesons off a proton bound in a deuteron target.
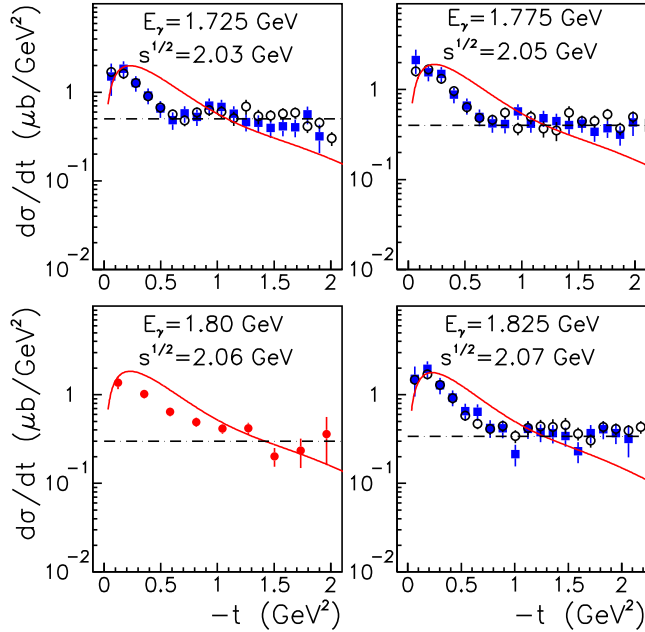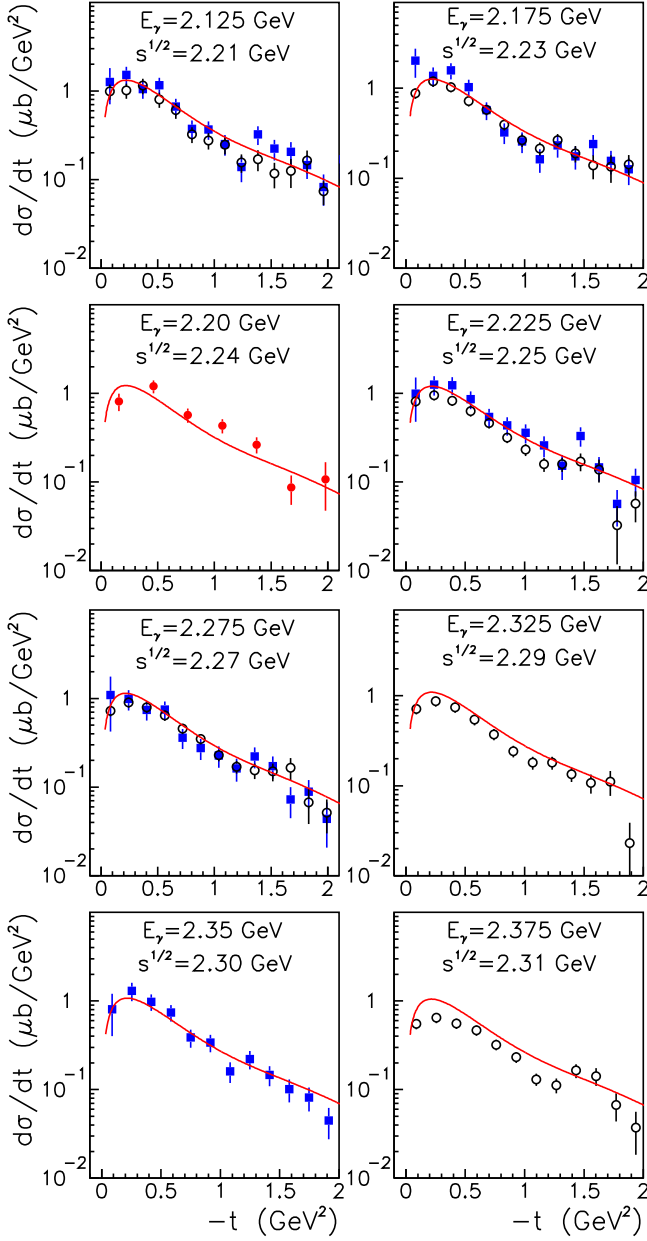

Fig. 1. Differential cross section for $\gamma p \to \eta p$ as a function of the four-momentum transfer squared at the photon energies E_γ (invariant collision energies $\sqrt{s}$) indicated in the figure. The data are collected at ELSA and published in 2005 [40] (filled squares), 2008 [41] (filled circles) and 2009 [1] (open circles). The solid lines are the results of our model. The dash-dotted lines indicate an estimation for the isotropic part of the differential cross section, cf. text.
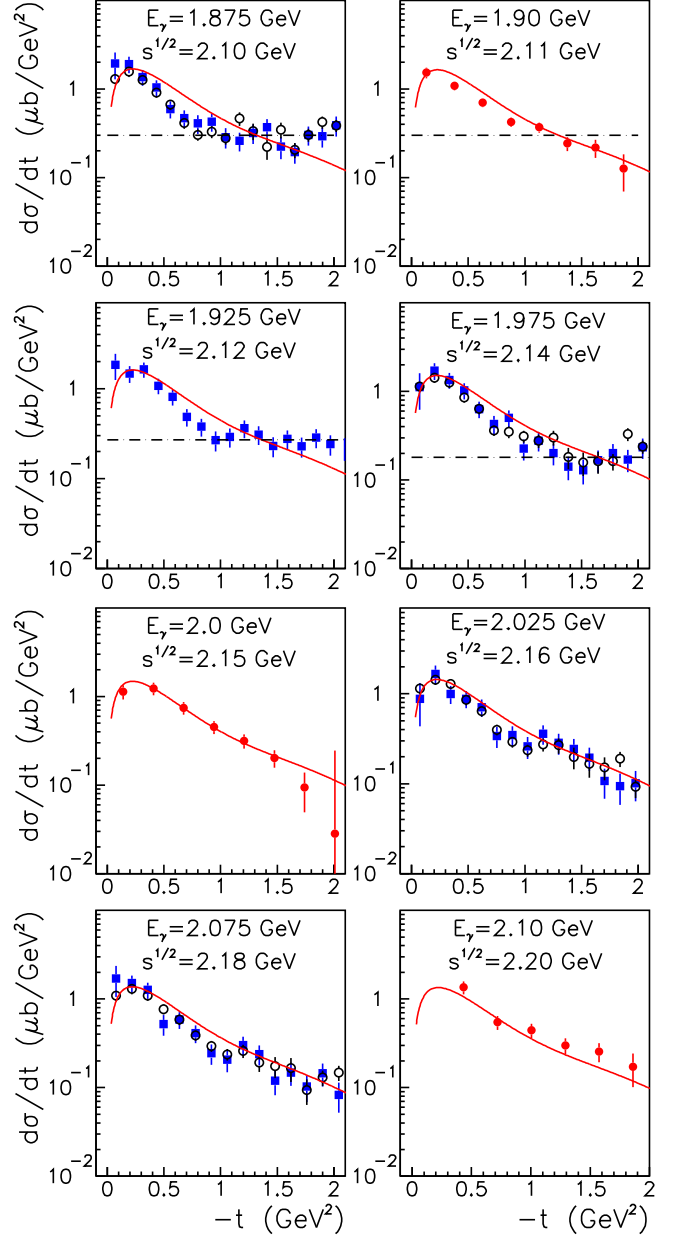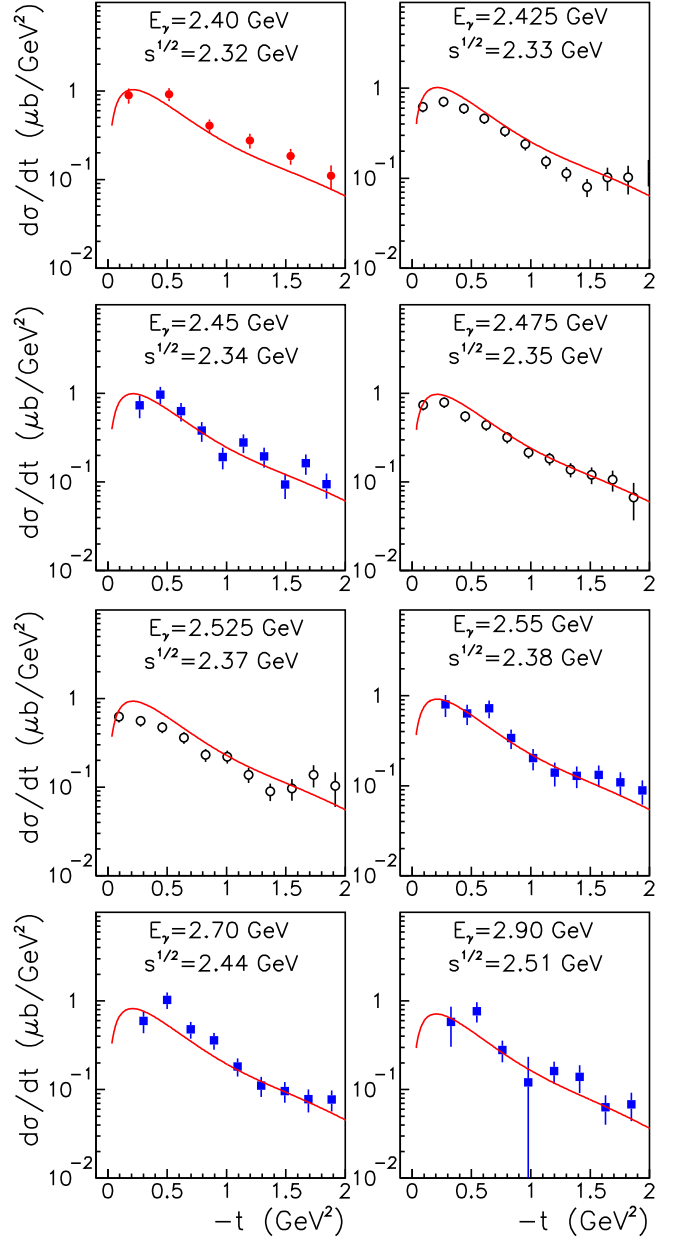

Fig. 2. Differential cross section for $\gamma p \to \eta p$. Same notation as in Fig. 1.

The results of our model are shown by solid lines. Obviously, these are in reasonable agreement with the data for invariant collision energies above 2.15 GeV, say. Note that the free parameters of the Regge model were fitted to $\gamma p \to \eta p$ data available at photon energies above 3 GeV. This means that the results shown here should be considered as predictions. Since we include only t-channel contributions, naturally one expects deviations of our results from the experiment when going to lower and lower energies, reflecting the increasing significance of additional contributions from s- and u-channel processes.

Interestingly, for energies $\sqrt{s} <$ 2.15 GeV the data indicate a peculiar feature. Namely, the differential cross

Fig. 3. Differential cross section for $\gamma p{\to}\eta p$. Same notation as in Fig. 1.

Fig. 4. Differential cross section for $\gamma p{\to}\eta p$. Same notation as in Fig. 1.

sections do not depend on the four-momentum transfer squared for $|t|$ above $\simeq 1.3$ GeV^2. Such an almost isotropic differential cross section is, in general, a sign for the excitation of an s-wave baryon resonance. The dash-dotted lines in Figs. 1 and 2 indicate our estimate for the isotropic part of the differential cross section which amounts to

$$\frac{d\sigma}{dt} = 0.5 \div 0.18 \ \mu\text{b/GeV}^2, \qquad (9)$$

and decreases slowly with energy within the range $2.03 \leq \sqrt{s} \leq 2.14$ GeV.

The observed isotropic behaviour might be an indication for the excitation of the $S_{11}(2090)$ resonance. Note,

however, that the latest GWU analysis [8] of πN scattering data found no evidence for this resonance, despite the fact that the $\pi^- p \to \eta n$ reaction was included in that analysis. Apparently, firm conclusions about a possible excitation of the $S_{11}(2090)$ baryon in the $\gamma p \to \eta p$ reaction require further analyses and not only data on differential cross section but also, and more importantly, polarization observables.

Finally, in Fig. 5 we present the total $\gamma p{\to}\eta p$ reaction cross section as a function of the invariant collision energy $\sqrt{s}$. To avoid a presentation with logarithmic scale we have multiplied the data as well as the model results with the leading Regge exponent (s^2). In case of the ELSA ex-
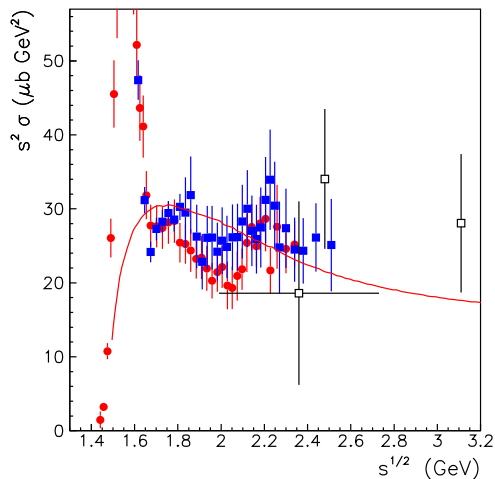
Fig. 5. Total reaction cross section for $\gamma p \rightarrow \eta p$ as a function of the invariant collision energy. The data are from ELSA from 2005 [40] (filled squares) and 2008 [41] (filled circles). Open squares are data collected in Ref. [42]. The line is the result of our Regge model. The data and the model results are multiplied by s^2.

periment the reaction cross section was obtained by summing over the angular bins and extrapolating outside the angular range of the actual measurement [40]. The filled squares show the ELSA results from 2005 [40] while the filled circles are those from 2008 [41]. Open squares are pre-2000 data collected in Ref. [42].

In view of the very large uncertainties of the ELSA results from 2005 [40] it is difficult to draw conclusions from the comparison between those data and the model calculation. However, it is obvious that the model results are at variance with the ELSA data from 2008 [41] for invariant collision energies around and below 2.15 GeV. This observation is in line with the shortcomings of the model with regard to the differential cross sections, discussed above.

In summary, we found mutual consistency between the $\gamma p \rightarrow \eta p$ measurements [1,40,41] available from ELSA. We observe a reasonable agreement between the results obtained in these three different ELSA experiments and our predictions at invariant collision energies above 2.15 GeV or photon energies $E_\gamma \geq 2$ GeV. Since the free parameters of our model were fixed in a fit to the pre-2000 data available at photon energies above 3 GeV, we conclude that there is also consistency between the ELSA data and the previous measurements performed at higher energies [36, 37,38,27,28].

4 CLAS measurements

The CLAS Collaboration has performed two different experiments for $\gamma p \rightarrow \eta p$ [2,12] at JLab. The data published in 2002 [12] cover invariant energies up to 2.12 GeV, while the most recent measurement [2] extends up to $\sqrt{s} \simeq 2.79$ GeV.

In Fig. 6 we present the data from the 2002 measurement [12] together with our model results. In view
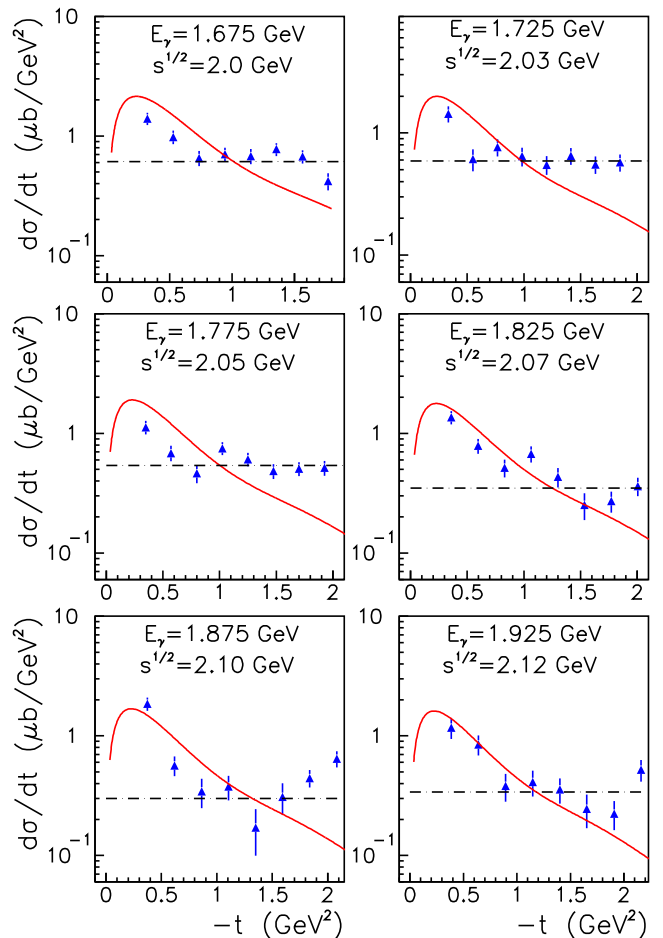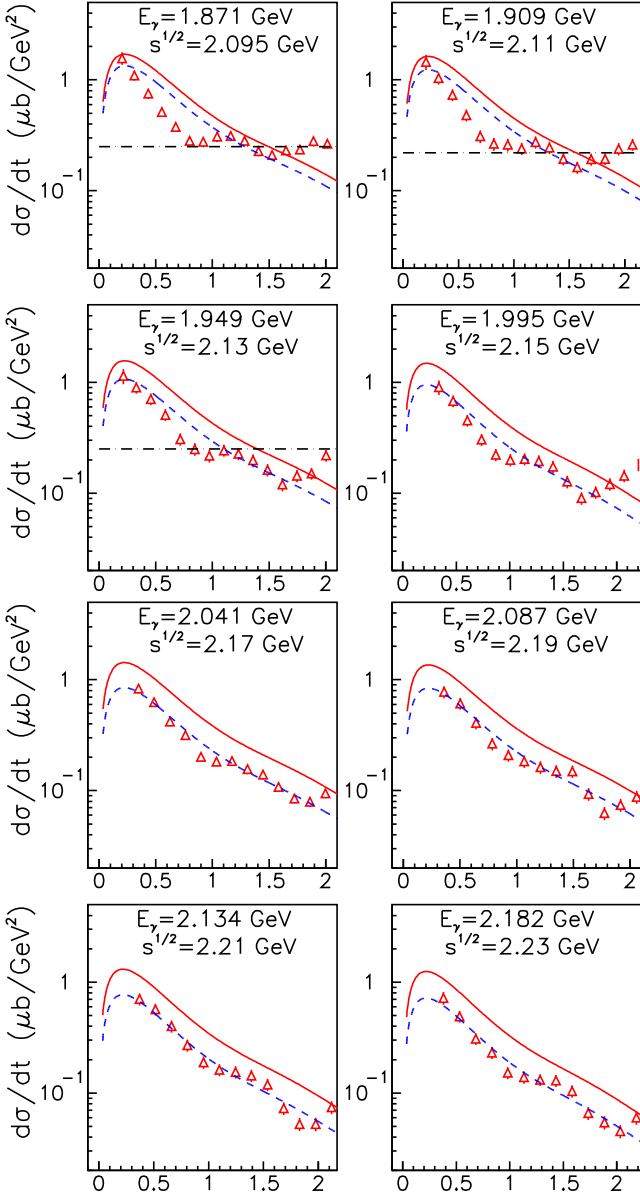

Fig. 6. Differential cross section for $\gamma p \rightarrow \eta p$ as a function of the four-momentum transfer squared at the photon energies E_γ (invariant collision energies $\sqrt{s}$) indicated in the figure. Filled triangles represent data by the CLAS Collaboration published in 2002 [12]. The solid lines are the results of our model. The dash-dotted lines indicate an estimation for the isotropic part of the differential cross section, cf. text.

of the disagreement with the ELSA data below $\sqrt{s} \approx 2.15$ GeV, reported in the last section, it is not surprising that the model prediction agrees only at the highest energy ($\sqrt{s}$=2.12 GeV) and for $|t| \leq 2$ GeV^2 roughly with the CLAS results, considering the large experimental uncertainties. At lower energy the $\gamma p \rightarrow \eta p$ differential cross sections show practically no t-dependence[1] for $|t|$ above $\simeq 1.3$ GeV^2. We illustrate this observation by the dash-dotted lines in the Fig. 6. These finding are in line with those for the ELSA data, discussed in the previous section.

The most recent results from CLAS [2] are displayed in Figs. 7-9. The plotted values for the data (triangles) are taken from the Durham data base [43]. An additional error of 11% in average was included in quadrature following the results given in Table 1 of Ref. [2]. It is clear

---

[1] Note that at large $|t|$ or small $|u|$ the experimental differential cross sections indicate some increase with $u \rightarrow 0$, which is typical for contributions from u-channel processes.

Fig. 7. Differential cross section for $\gamma p \rightarrow \eta p$ as a function of the four-momentum transfer squared at the photon energies E_γ (invariant collision energies $\sqrt{s}$) indicated in the figure. Open triangles represent data by the CLAS Collaboration published in 2009 [2]. The solid lines are the results of our model. When allowing the normalization to float the dashed lines are obtained. The dash-dotted lines shown in the plots for $E_\gamma \leq$ 1.949 GeV indicate an estimation for the isotropic part of the differential cross section, cf. text.

Fig. 8. Differential cross section for $\gamma p \rightarrow \eta p$. Same notation as in Fig. 7.

that the experimental results are in strong disagreement with our calculation which are indicated by the solid lines. The discrepancy is especially surprising for invariant energies above 2.54 GeV or $E_\gamma > 3$ GeV. As said before, the parameters of our model were fixed [11] utilizing the data on differential cross sections and polarization available at photon energies above 3 GeV. Thus, the observed
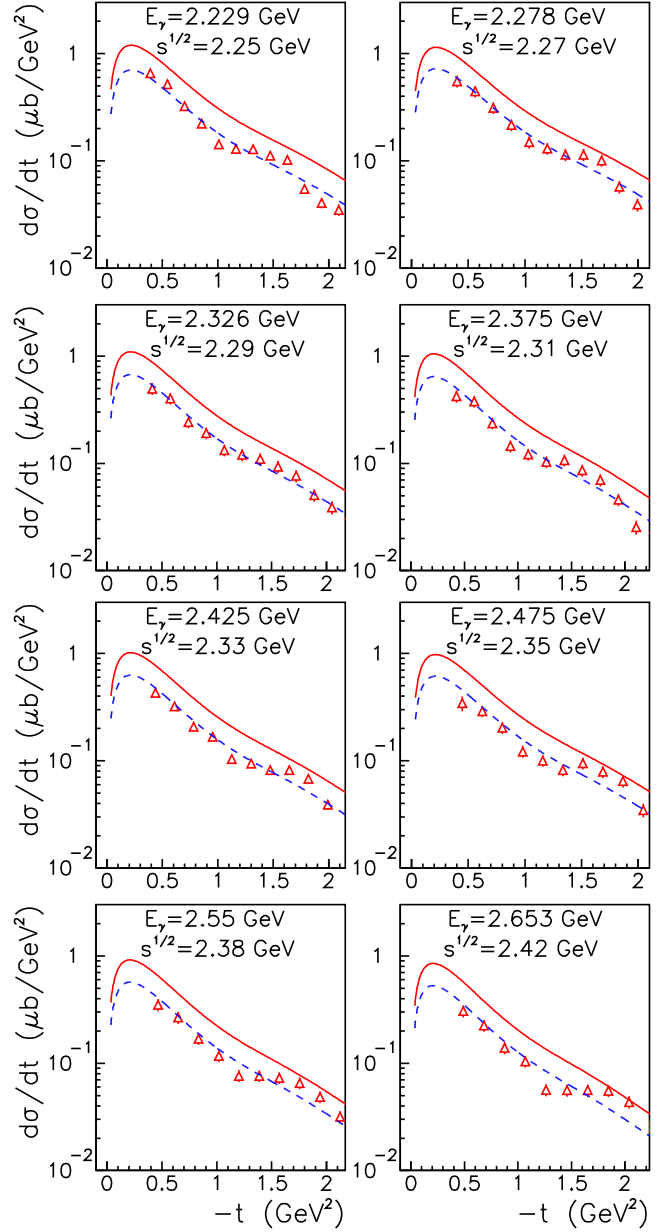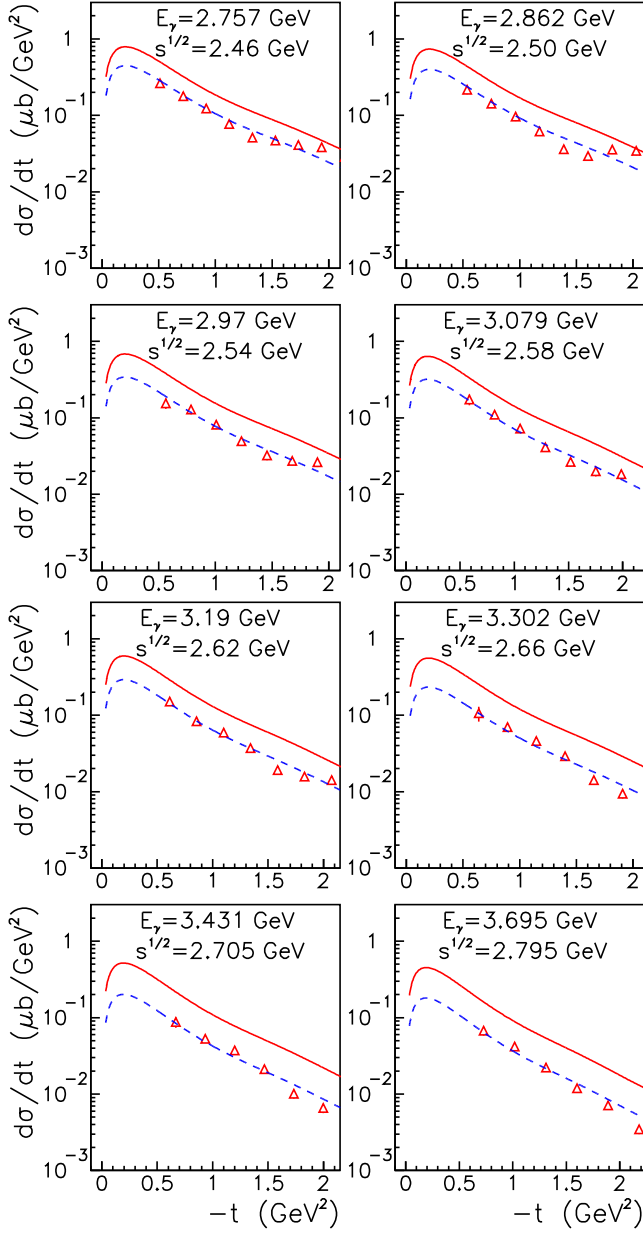
disagreement means that the new CLAS results are inconsistent with the pre-2000 measurements [36,37,38,27, 28] from SLAC, DESY, Cornell and the Daresbury laboratory. But they are also inconsistent with the three sets of measurements [1,40,41] from ELSA, and the 2002 results from the CLAS collaboration itself [12].

5 Comparison of the different data sets

A direct comparison of the different measurements is difficult because, in general, the ELSA and CLAS data are available at different energies and different angles. In the
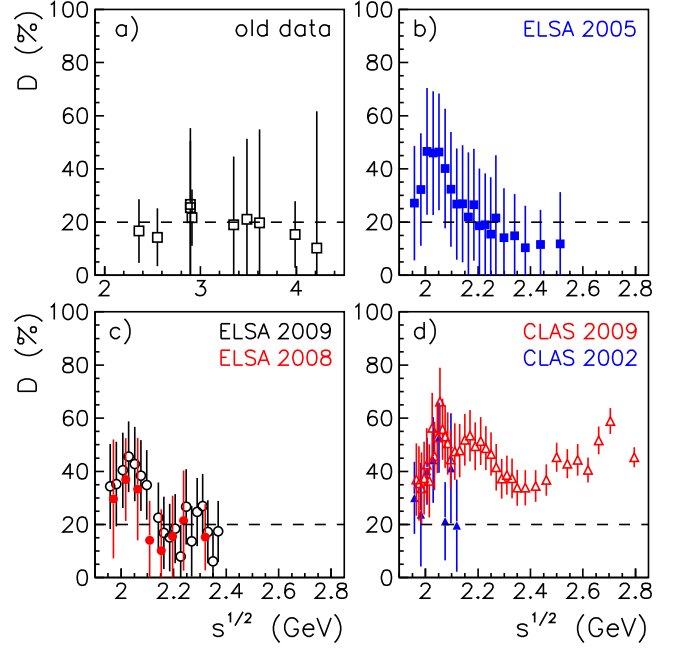
Fig. 9. Differential cross section for $\gamma p \to \eta p$. Same notation as in Fig. 7
.

Fig. 10. The deviation D as a function of invariant collision energy $\sqrt{s}$ shown for different experiments: pre-2000 measurements (open squares), ELSA measurements from 2005 [40] (filled squares), 2008 [41] (filled circles), 2009 [1] (open circles) and CLAS measurements from 2002 [12] (filled triangles), 2009 [2] (open triangles). The dashed lines indicate an averaged D value obtained with pre-2000 data.

present study we circumvent this problem by comparing the experimentally observed differential cross sections with the predictions of our Regge model [11].

For the following discussion let us define a function D as a measure of the discrepancy (or deviation) of the experimental results for the η-meson photoproduction differential cross section from our model results:

$$D(\sqrt{s}) = \frac{1}{N} \sum_{i=1}^{N} \frac{|(d\sigma/dt)_i^{\mathrm{exp}} - (d\sigma/dt)_i^{\mathrm{th}}|}{(d\sigma/dt)_i^{\mathrm{exp}}} . \qquad (10)$$

The summation is done over all data points in the range of the four-momentum transfer squared $t \geq -2$ GeV^2 at fixed invariant collision energy $\sqrt{s}$, and N is the number of experimental points at each energy. Here $(d\sigma/dt)_i^{\mathrm{exp}}$ stands for the experimental value while $(d\sigma/dt)_i^{\mathrm{th}}$ denotes the result of our Regge model for the ith data point at a specific energy $\sqrt{s}$. In practice, Eq. (10) represents the relative uncertainty of our model with respect to the data averaged over the t-distribution or, alternatively, over the angular spectrum at a fixed energy. We do not include polarization data since there are only few data points and, moreover, the data at two photon energies are afflicted by large uncertainties.

To indicate the uncertainties of the experimental values we consider a relative error averaged over the t-spectrum at each energy, which is given by

$$\delta D(\sqrt{s}) = \frac{1}{N} \sum_{i=1}^{N} \frac{\sqrt{(\Delta_i^{\mathrm{stat}})^2 + (\Delta_i^{\mathrm{sys}})^2}}{(d\sigma/dt)_i^{\mathrm{exp}}} . \qquad (11)$$

Here Δ^{stat} and Δ^{sys} are the absolute statistical and systematical experimental uncertainties given for the ith data point. They are combined in quadrature similar to the pion data analysis performed in Ref. [8].

It is useful to consider another quantity that was introduced in Refs. [9,10] for the evaluation of the consistency of data for the $\gamma p \to K^+ \Lambda$ reaction. The deviation of each data point from the model result was computed from

$$R_i = \frac{(d\sigma/dt)_i^{\mathrm{exp}} - (d\sigma/dt)_i^{\mathrm{th}}}{\Delta\sigma_i^{\mathrm{stat}}}, \qquad (12)$$

with the mean value $\langle R \rangle$ and second algebraic moment $\langle R^2 \rangle$ defined by

$$\langle R \rangle = \frac{1}{N} \sum_{i=1}^{N} R_i, \qquad (13)$$
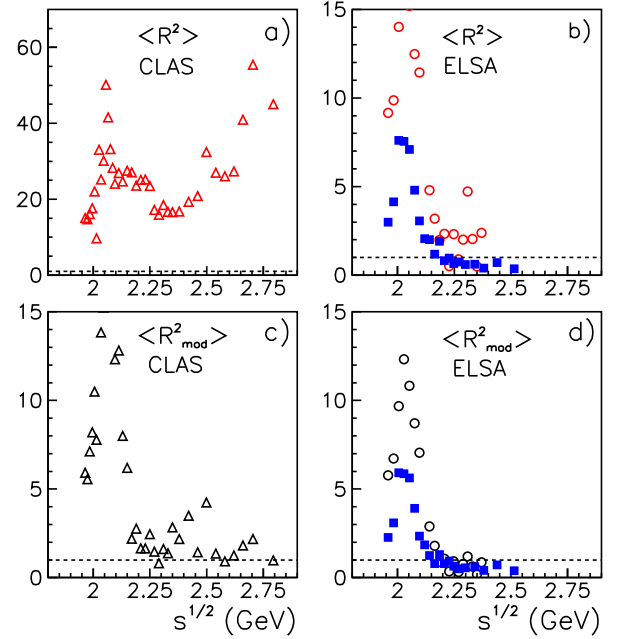
$$\langle R^2 \rangle = \frac{1}{N} \sum_{i=1}^{N} R_i^2 = \frac{\chi^2}{N}. \qquad (14)$$

As indicated, the quantity $\langle R^2 \rangle$ is equivalent to the standard χ^2 per data point. The evaluation of R_i involves the statistical uncertainty of the data points, which can be very different for different measurements. Thus, it can happen that the relative deviation is large, but due to small values of $\Delta\sigma_i^{\text{stat}}$ and not because of a substantial difference between model predictions and the data. This has to be taken into account in the interpretation of the results for R_i, etc. In the present study we will show the energy dependence of the second moment $\langle R^2 \rangle$ in order to illustrate the role of the statistical uncertainties of the experimental results.

Results for $D(\sqrt{s})$, evaluated for the pre-2000 data [36, 37, 38, 27, 28] on $\gamma p \to \eta p$, are shown in Fig. 10a). Note that the deviation presented in Fig. 10 is given in percent. From the results in Fig. 10a) we conclude that the deviation of the model calculation from those pre-2000 experimental results amounts to about 20% in average. The dashed line represents this average value and is shown in all panels in Fig. 10 for illustrative purposes. This deviation is well within the uncertainties of the experimental data as is reflected by the fact that the error bars, corresponding to the variation δD, cross the zero-percent line in most of the cases.
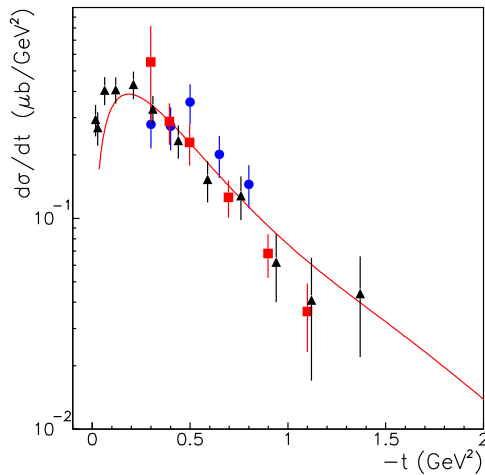
**Fig. 12.** The second moment of the deviation $\langle R^2 \rangle$, cf. Eq. (14), evaluated for the 2009 CLAS data [2] (open triangles) and the ELSA data from 2009 [1] (open circles) and 2005 [40] (filled squares). The dashed lines indicate $\langle R^2 \rangle = 1$. In panels a) and b) we show results for the data as published, while in c) and d) the modified $\langle R_{\text{mod}}^2 \rangle$ that involves the renormalization factor X are presented.

One could believe that the deviation D can be further minimized, e.g., by renormalizing the model results[2]. But this is not the case because from a certain level onwards D provides only a measure for the reproduction of the t-dependence. This is well illustrated by Fig. 11 where the differential cross section for $\gamma p \to \eta p$ at the photon energy of 4 GeV is displayed. Indeed an overall normalization would not improve the description of the data since the t-dependence is an essential feature of the model as well as of the data.

Fig. 10b) summarises the deviation between our calculation and the results from the ELSA experiment published [40] in 2005. The values of the cross sections and the error bars were taken from the Durham data base. In the evaluation of the relative uncertainties δD we include the statistical and systematic errors as given in the Tables in Refs. [40,43] and, in addition, we add in quadrature a normalization error of 15%.

The agreement between the data and the model at energies $\sqrt{s} > 2.15$ GeV is quite reasonable, as expected from the comparison presented in Sect. 3. At these energies the relative deviation amounts in average to $\simeq 7\%$, which is compatible with the experimental uncertainties. For lower energies the deviation increases and it reaches a maximum

Fig. 11. Differential cross section for $\gamma p \to \eta p$ as a function of the four-momentum transfer squared at the photon energy of 4 GeV. The squares represent data from SLAC [36], triangles are from DESY [37] and circles are from Cornel [38]. The solid line is the result of our model.

---

[2] Actually we use a χ^2 minimization procedure to find an optimal description of the data. In this case we also account for the uncertainty of each experimental point. Note that the definition of the χ^2 differs from that of the quantity D.
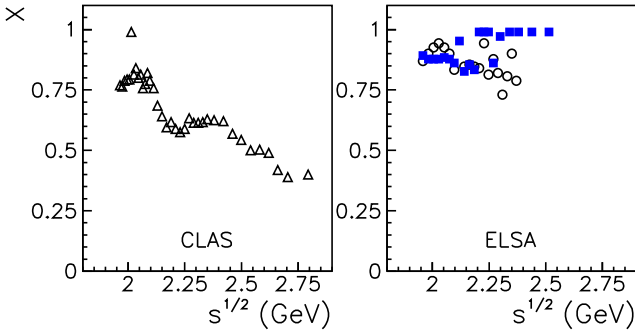
Fig. 13. Renormalization factor X as a function of the invariant collision energy. Open triangles represent the values obtained in the analysis of the CLAS data [2], while the open circles and filled squares are for the ELSA measurements from 2009 [1] and 2005 [40], respectively.

value of about 45% around invariant energies of 2.1 GeV. Interestingly, the result for D resembles pretty much a distribution one would expect for a resonance structure.

Results for the more recent data from ELSA [41,1] published in 2008 and 2009 are summarized in Fig. 10c). Again the values for the differential cross section and the statistical and systematic uncertainties were taken from data base [43]. These errors were added quadratically to obtain the total error as indicated by Eq. (11). The systematic uncertainty of the 2008 data [41] was assumed to be 10% at photon energies below 2 GeV and 15% at higher photon energies. We find that there is also a good overall agreement between the model calculation and both sets of the recent ELSA measurements at $2.15 < \sqrt{s} < 2.4$ GeV. At these energies the relative deviation amount to an average of $\simeq 5\%$, which is less than the experimental uncertainties. For lower energies the deviation increases and reaches values around 40% for $\sqrt{s} \simeq 2.1$ – similar to what was found for the 2005 data from the ELSA collaboration.

Finally, in Fig. 10d) the deviation D between our model result and the experimental data [12,2] from CLAS is shown. With respect to the 2002 data [12] the overall normalization uncertainty was estimated to be in the range of 3% to 7%, increasing with photon energy. For the data published in 2009 [2] an additional average error of 11% was included in quadrature following the results given in Table 1 of Ref. [2].

The few data points from the 2002 measurements [12] at invariant collision energies above $\simeq 2.1$ GeV are reasonably well described by the model. However, the very recent CLAS results [2] deviate substantially from the model over the whole range of $2.1 < \sqrt{s} < 2.8$ GeV, *i. e.* for energies where we observe good agreement with all other experimental results. Taking into account the systematic uncertainties shows that the two CLAS measurements [12, 2] themselves are not consistent with each other.

In the following let us investigate whether the observed significant discrepancy with the new CLAS data could be resolved by changing the absolute normalization of those data. In fact, the results displayed in Figs. 7-9 suggest that for $\sqrt{s} \geq 2.54$ GeV the shape of the t-dependence exhibited

by the CLAS data looks indeed very similar to our model predictions. For that purpuse we consider a modified χ^2 function given by

$$\chi^2_{mod} = \sum_i^N \left[\frac{(d\sigma/dt)_i^{\mathrm{exp}} - X(d\sigma/dt)_i^{\mathrm{th}}}{\Delta\sigma_i^{\mathrm{stat}}} \right]^2 \qquad (15)$$

and evaluate the renormalization factor X at each energy by searching for the minumum of χ^2_{mod}. The quantity χ^2_{mod} should be compared with the second moment of the deviation $\langle R^2 \rangle$ given by Eq. (14), specifically, we can introduce $\langle R^2_{\mathrm{mod}} \rangle = \chi^2_{\mathrm{mod}}/N$.

The open triangles in Fig. 12a) show $\langle R^2 \rangle$ as a function of the invariant collision energy evaluated for the 2009 data [2] from CLAS. Apparently the discrepancy between our model and the data is huge, even at $\sqrt{s} > 2.25$ GeV. This result is rather different from the $\langle R^2 \rangle$ evaluation for the ELSA data presented in Fig. 12b). Besides the 2009 results [1] (open circles) we consider here also the ELSA results from 2005 [40] (filled squares). The latter measurement is afflicted with somewhat larger uncertainties but it covers higher energies and, therefore, is interesting too for the present systematic analysis. Note that a different scale is used in Fig. 12a), i.e. for the results corresponding to the CLAS data.

After floating the normalization for the CLAS data from 2009 the agreement between experiment and the model predictions improves significantly. This is illustrated in Fig. 12c). Specifically, for $\sqrt{s} > 2.25$ GeV the values for $< R^2_{\mathrm{mod}} >$ (i.e. the χ^2 per data point) are now, in general, within the range of 1–2. In case of the ELSA data floating the normalization has an influence too, but it is much less dramatic. Basically, the χ^2 which amounted to values around 2 for energies above 2.25 GeV improves further to values around 1. Thus, once the normalization of the CLAS data is allowed to float there is a comparable agreement of our model result with the CLAS 2009 and with the ELSA measurements. This suggests that all data available for the $\gamma p \rightarrow \eta p$ differential cross section are indeed mutually consistent, at least as far as their t-dependence is concerned.

The renormalization factor X is presented in Fig. 13 as a function of the invariant collision energy. As can be seen, for the CLAS data X is not constant. It depends considerably on the energy in a rather peculiar though still fairly smooth way. At the highest energy measured by the CLAS collaboration more than a factor two is required to bring their data in agreement with the measurements at higher energies. In case of the ELSA 2009 data the normalization factor shows deviations in the order of 15% from the nominal value 1. Interestingly, one can see several strong statistical fluctuations. For the ELSA 2005 data the normalization factor differs even less from 1. In fact, for the higher energies X is practically identical to the nominal value.

More details about this statistical analysis are summarized in an Appendix. Specifically, there we provide numerical values for the achieved χ^2 and the normalization factor X at each energy of the CLAS 2009 and the ELSA 2005 and 2009 measurements.

Let us come back once again to the CLAS 2009 data. The dashed curves in Figs. 7-9 indicate results where the renormalization factor is taken into account. Now there is a reasonable overall agreement between the experiment [2] and the model calculation. It is worth noting that there are some remaining deviations at two ranges of the invariant collision energy. At $2.09 \leq \sqrt{s} \leq 2.13$ GeV the data clearly show a t-independent behaviour at $|t|$ above 1.3 GeV^2, say, which is illustrated by the dash-dotted lines. This observation is in line with the finding from the analysis of the ELSA data and might reflect the excitation of the $S_{11}(2090)$ resonance. Furthermore, at the energy range $2.31 \leq \sqrt{s} \leq 2.54$ GeV the experimental results show some structure at $|t| \geq 1.3$ GeV^2. Hints for such a structure are also seen in the ELSA data from 2009, cf. Figs. 1 and 2. This could be a reflection of an excitation of a high spin resonance.

In the context of the issues discussed in this section let us mention a recent analysis of the $\gamma p \to \eta p$ reaction given in Ref. [44]. The conclusion of that study was that the recently published data by CLAS and ELSA in the energy range $1.6 \leq \sqrt{s} \leq 2.8$ GeV are well reproduced due to the inclusion of Reggeized trajectories instead of simple ρ and ω poles. Obviously, our systematic analysis of η-meson photoproduction results does not support this statements from Ref. [44] but reaches a different conclusion.

6 Summary

We performed a systematic analysis of data available for differential cross sections of the reaction $\gamma p \to \eta p$. In particular, we addressed the issue of consistency between the most recent data published by the ELSA [1] and CLAS [2] collaborations. Since the two measurements produced data points that are, in general, at different energies and four-momentum transfer squared or angles it is difficult to compare them directly. Therefore, we utilized here as a link results of our Regge model that was fitted previously [11] to the η-photoproduction data (differential cross sections and polarizations) at photon energies above 3 GeV ($\sqrt{s} > 2.55$ GeV) [36,37,38,27,28]. Note that the latter aspect implies that our results may be considered as predictions with regard to the ELSA [1] and CLAS [2] measurements.

It was found out that our model reproduces the ELSA data from 2005 [40], from 2008 [41], and from 2009 [1] as well as the CLAS results published in 2002 [12] fairly well down to $\sqrt{s} \simeq 2.15$ GeV. At the same time we detected a substantial discrepancy between the model calculations and the new CLAS data from 2009 [2]. When floating the normalization of the new CLAS data it was possible to obtain a quite reasonable description of those data and bring them in line with our analysis of the other measurements. Indeed such a renormalization leads to a mutual consistency of all the $\gamma p \to \eta p$ data available presently for the differential cross sections at invariant collision energies above approximately 2 GeV. It turns out, however, that the renormalization factor depends on the energy. Specifically, it increases more or less smoothly with energy and

amounts to more than a factor two at the highest energy measured by the CLAS collaboration in 2009.

As a by-product we found promising indications for the presence of the $S_{11}(2090)$ excited baryon in form of an almost constant differential cross section at $|t| > 1.3$ GeV^2 within the range $2.03 \leq \sqrt{s} \leq 2.14$ GeV. This observation is based on both the ELSA and CLAS measurements. We also detected hints for a resonance-like structure at the energy range $2.31 \leq \sqrt{s} \leq 2.54$ GeV covered by the CLAS data [2].

7 Appendix

In this Appendix we provide quantitative details of the comparison of our model results with the data from the CLAS 2009 and the ELSA 2005 and 2009 measurements. Specifically, we list the χ^2, for the original data points as well as after introducing a free normalization X at each of the measured energies. The definition of the normalization constant X and of the χ^2 is given in Eq. (15). The χ^2 is obtained by considering all available data points in the range $|t| \leq 2$ GeV^2. We performed also fits to a smaller t range, namely for $|t| \leq 1$ GeV^2, guided by the idea that our Regge model might be even more reliable for such small t values. However, since often just 2 or 3 data points lie within that range we refrain from giving a corresponding χ^2 here. Rather we use the X obtained from the smaller t range as an error estimate. The difference between the X values obtained for the two t ranges is quoted as uncertainty in Tables 4 - 6.

Results for the CLAS 2009 data are given in Table 4. Comparing columns 3 and 5 one can see the dramatic improvement in the description once a normalization factor is introduced. Furthermore, the difference between the CLAS data and the high-energy data, as represented by our Regge model is large. It amounts to a factor of 2 and more for invariant collision energies above 2.50 GeV. When floating the normalization the χ^2 reduces to values around 1 to 2, which indicates that the t dependence found in the CLAS 2009 experiment is well in line with the one exhibited by the high-energy data (and the Regge model). The χ^2 is somewhat larger between 2.31 and 2.5 GeV where there are indications for some structure in the t dependence of the CLAS data that is not in line with the Regge prediction, cf. the discussion in Sect. 5. For invariant collision energies below 2.15 GeV, say, the χ^2 improves only moderately when floating the normalization and remains fairly large indicating the fact that our Regge model

is no longer able of describing the t dependence of the data. As expected, such a shortcoming cannot be compensated by floating the normalization factor X. Moreover, then the value for X depends strongly on whether we fit the data up to t=-1 GeV^2 or -2 GeV^2, cf. the corresponding uncertainty given in the table.

In case of the ELSA 2009 data there is also an improvement in the χ^2 when we float the normalization, cf. Table 5. However, the change is by far not as dramatic as for the CLAS 2009 data. Indeed, in general, the normalization factor turns out to be within 10 to 20% only. Also here we see an increasing deviation of the model predictions from the t dependence of the data for energies below 2.15 GeV.

The ELSA 2005 measurement provided data for somewhat higher energies than the one from 2009. Interestingly, those data are in perfect agreement with the normalization of our Regge model, fixed from older data for $\gamma p \to \eta p$ at higher energies. The normalization factor found for the range 2.30 - 2.50 GeV is practically identical to 1, cf. Table 6. Again we see an increasing deviation of the model predictions from the t dependence of the data for energies below 2.15 GeV.

References

1. V. Crede *et al.*, Phys. Rev. C **80**, 055202 (2009).
2. M. Williams *et al.*, Phys. Rev. C **80**, 045213 (2009).
3. S. Ceci, A. Švarc and B. Zauner, Phys. Rev. Lett. **97**, 062002 (2006).
4. A. V. Sarantsev *et al.*, Phys. Lett. B **659**, 94 (2008) [arXiv:0707.3591 [hep-ph]].
5. J.R. Bergervoet, P.C. van Campen, W.A. van der Sanden and J.J. de Swart, Phys. Rev. C **38**, 15 (1988).
6. R. Timmermans, T.A. Rijken and J.J. de Swart, Phys. Rev. C **50**, 48 (1994).
7. R.A. Arndt and L.D. Roper, Nucl. Phys. B **50**, 285 (1972).
8. R.A. Arndt, W.J. Briscoe, I.I. Strakovsky and R.L. Workman , Phys. Rev. C **74**, 045205 (2006).
9. R.A. Adelseck and B. Saghai, Phys. Rev. C **42**, 108 (1990).
10. P. Bydžovský and T. Mart, Phys. Rev. C **76**, 065202 (2007).
11. A. Sibirtsev, J. Haidenbauer, S. Krewald and U.-G. Meißner, Eur. Phys. J. A **44**, 169 (2010).
12. M. Dugger *et al.*, Phys. Rev. Lett. **89**, 222001 (2002).
13. A. Sibirtsev, J. Haidenbauer, S. Krewald, T.-S.H. Lee, U.-G. Meißner and A.W. Thomas, Eur. Phys. J. A **34**, 49 (2007).
14. A. Sibirtsev, J. Haidenbauer, S. Krewald and U.-G. Meißner, Eur. Phys. J. A **41**, 71 (2009).
15. C. Amsler *et. al.* (Particle Data Group), Phys. Lett. B **667**, 1 (2008).
16. T.P. Vrana, S.A. Dytman and T.-S.H. Lee, Phys. Rept. **328**, 181 (2000).
17. M. Batinic, I. Slaus, A. Švarc and B.M.K. Nefkens, Phys. Rev.C **51**, 2310 (1995).
18. R. E. Cutkosky, C. P. Forsyth, R. E. Hendrick and R. L. Kelly, Phys. Rev. D **20**, 2839 (1979).
19. R. Koch and E. Pietarinen, Nucl. Phys. A **336**, 331 (1980).
20. G. Höhler, *Landolt-Börnstein New Series, Group I, Elementary particles, Nuclei and Atoms,* Vol. **9b1** (Springer, Berlin, 1983).
21. A. Sibirtsev, J. Haidenbauer, S. Krewald and U.-G. Meißner, Eur. Phys. J. A **34**, 49 (2007).
22. A. C. Irving and R. P. Worden, Phys. Rept. **34**, 117 (1977).

Table 4. Comparison of the CLAS data from 2009 [2] with the results of our Regge model for $|t| \leq 2$ GeV^2 at different photon energies E_γ. Values for the χ^2/N based on the published data are given in the third column. The renormalization factor X obtained in a modified χ^2 fit, cf. Eq. (15), is given in the fourth column while the corresponding χ^2/N can be found in the fifth column. The uncertainty of X is explained in the text.

E_γ (GeV)	$\sqrt{s}$ (GeV)	χ^2/N	X	χ^2_{mod}/N
3.695	2.79	45.0	0.40±0.03	1.0
3.431	2.70	55.4	0.39±0.03	2.2
3.302	2.66	41.0	0.42±0.04	1.8
3.190	2.62	27.3	0.47±0.03	0.9
3.079	2.58	26.1	0.50±0.04	0.9
2.970	2.54	27.0	0.50±0.02	1.4
2.862	2.50	32.4	0.50±0.01	1.9
2.757	2.46	20.9	0.57±0.02	1.4
2.653	2.42	19.4	0.59±0.03	2.4
2.550	2.38	16.8	0.63±0.06	2.2
2.475	2.35	16.6	0.63±0.09	2.8
2.425	2.33	16.7	0.62±0.04	1.4
2.375	2.31	18.5	0.61±0.06	1.6
2.326	2.29	15.9	0.61±0.04	0.8
2.278	2.27	17.2	0.63±0.02	1.5
2.229	2.25	23.5	0.60±0.03	2.2
2.182	2.23	25.2	0.58±0.03	1.6
2.134	2.21	25.1	0.59±0.00	1.6
2.087	2.19	23.6	0.60±0.03	1.7
2.041	2.17	27.0	0.60±0.05	2.2
1.995	2.15	27.5	0.61±0.07	3.7
1.949	2.13	24.7	0.64±0.10	4.8
1.909	2.11	26.9	0.71±0.17	10.0
1.871	2.10	24.1	0.75±0.21	10.3
1.848	2.08	28.2	0.78±0.25	14.0
1.826	2.07	33.2	0.74±0.26	14.2
1.804	2.06	41.6	0.72±0.25	16.6
1.782	2.05	50.2	0.81±0.36	24.0
1.760	2.04	30.2	0.80±0.27	15.2
1.738	2.03	25.2	0.83±0.29	13.2
1.717	2.03	33.0	0.81±0.30	16.9
1.695	2.01	9.7	0.99±0.27	7.8
1.674	2.01	22.0	0.79±0.20	10.5
1.653	2.00	17.6	0.79±0.17	8.2
1.631	1.98	16.1	0.79±0.15	7.1
1.610	1.97	14.8	0.76±0.12	5.5
1.589	1.96	15.1	0.77±0.12	5.9

Table 5. Comparison of the ELSA data from 2009 [1] with the results of our Regge model for $|t| \leq 2$ GeV^2 at different photon energies E_γ. Values for the χ^2/N based on the published data are given in the third column. The renormalization factor X obtained in a modified χ^2 fit, cf. Eq. (15), is given in the fourth column while the corresponding χ^2/N can be found in the fifth column. The uncertainty of X is explained in the text.

E_γ (GeV)	$\sqrt{s}$ (GeV)	χ^2/N	X	χ^2_{mod}/N
2.525	2.37	2.4	0.79±0.06	0.9
2.475	2.35	0.5	0.90±0.03	0.2
2.425	2.33	2.0	0.81±0.00	0.6
2.375	2.31	4.7	0.73±0.01	1.2
2.325	2.29	2.0	0.82±0.00	0.8
2.275	2.27	0.9	0.88±0.00	0.3
2.225	2.25	2.3	0.81±0.03	0.9
2.175	2.23	0.5	0.94±0.03	0.4
2.125	2.21	2.3	0.84±0.01	1.1
2.075	2.18	2.0	0.85±0.00	0.9
2.025	2.16	3.2	0.85±0.01	1.8
1.975	2.14	4.8	0.85±0.06	2.9
1.875	2.10	11.4	0.83±0.13	7.1
1.825	2.07	12.5	0.90±0.20	8.7
1.775	2.05	15.2	0.93±0.24	10.8
1.725	2.03	17.7	0.94±0.26	12.3
1.675	2.01	14.0	0.93±0.21	9.7
1.625	1.98	9.9	0.90±0.14	6.7
1.575	1.96	9.2	0.87±0.10	5.8

Table 6. Comparison of the ELSA data from 2005 [40] with the results of our Regge model for $|t| \leq 2$ GeV^2 at different photon energies E_γ. Values for the χ^2/N based on the published data are given in the third column. The renormalization factor X obtained in a modified χ^2 fit, cf. Eq. (15), is given in the fourth column while the corresponding χ^2/N can be found in the fifth column. The uncertainty of X is explained in the text.

E_γ (GeV)	$\sqrt{s}$ (GeV)	χ^2/N	X	χ^2_{mod}/N
2.900	2.51	0.4	0.99±0.00	0.4
2.700	2.44	0.7	0.99±0.00	0.7
2.550	2.38	0.4	0.99±0.00	0.4
2.450	2.34	0.6	0.99±0.00	0.6
2.350	2.30	0.6	0.97±0.02	0.6
2.275	2.27	0.8	0.86±0.01	0.5
2.225	2.25	0.7	0.99±0.00	0.6
2.175	2.23	1.0	0.99±0.00	0.9
2.125	2.21	0.8	0.99±0.00	0.8
2.075	2.18	1.9	0.83±0.03	1.3
2.025	2.16	1.2	0.85±0.05	0.8
1.975	2.14	2.0	0.83±0.01	1.3
1.925	2.12	2.1	0.95±0.14	1.9
1.775	2.05	7.1	0.88±0.23	5.6
1.875	2.10	3.1	0.86±0.11	2.3
1.825	2.07	4.8	0.88±0.18	3.9
1.725	2.03	7.6	0.88±0.24	5.9
1.675	2.01	7.6	0.88±0.21	5.9
1.625	1.98	4.1	0.88±0.17	3.1
1.575	1.96	3.0	0.89±0.14	2.3

23. P.D.B. Collins, *An Introduction to Regge Theory and High Energy Physics*, Cambridge University, Cambridge, England (1977) 275.
24. B. H. Kellett, Nucl. Phys. B **25**, 205 (1970).
25. M. Guidal, J.M. Laget and M. Vanderhaeghen, Nucl. Phys. A **627**, 645 (1997).
26. M. Vanderhaeghen, M. Guidal and J.M. Laget, Phys. Rev. C **57**, 1454 (1998).
27. P.J. Bussey *et al.*, Phys. Lett. B **61**, 479 (1976).
28. P.J. Bussey *et al.*, Nucl. Phys. B **185**, 269 (1981).
29. F. Huang, A. Sibirtsev, S. Krewald, C. Hanhart, J. Haidenbauer, Ulf-G. Meißner, Eur. Phys. J. A **44**, 81 (2010).
30. A. Sibirtsev, K. Tsushima and S. Krewald, Phys. Rev. C **67**, 055201 (2003).
31. A. Sibirtsev, J. Haidenbauer, F. Huang, S. Krewald and Ulf-G. Meißner, Eur. Phys. J. A **40**, 65 (2009).
32. M. Rahnama and J. K. Storrow, J. Phys. G **17**, 243 (1991).
33. J. N. J. White, Phys. Lett. B **26**, 461 (1968).
34. J. N. J. White, Nucl. Phys. B **13**, 139 (1969).
35. F. Henyey, G. L. Kane, Jon Pumplin and M. H. Ross, Phys. Rev. **182**, 1579 (1969).
36. R.L. Anderson *et al.*, Phys. Rev. D **1**, 27 (1970).
37. W. Braunschweig *et al.*, Phys. Lett. B **33**, 236 (1970).
38. J. Dewire, B. Gittelman, R. Loe, E.C. Loh, D.J. Ritchie and R.A. Lewis, Phys. Lett. B **37**, 326 (1971).
39. H. Primakoff, Phys. Rev. **81**, 899 (1951).
40. V. Crede *et al.*, Phys. Rev. Lett. **94**, 012004 (2005).
41. I. Jaegle *et al.*, Phys. Rev. Lett. **100**, 252002 (2008).
42. *Landolt-Börnstein New Series, Group I, Elementary particles, Nuclei and Atoms,* Vol. **8** (Springer, Berlin, 1983).
43. The Durham HepData Project, http://hepdata.cedar.ac.uk
44. J. He and B. Saghai, arXiv:1005.2797 [nucl-th].